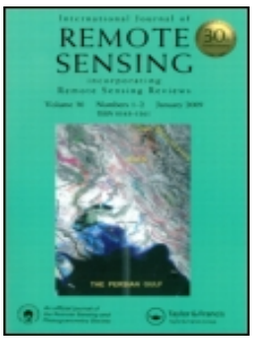

International Journal of Remote Sensing

ISSN: 0143-1161 (Print) 1366-5901 (Online) Journal homepage: https://www.tandfonline.com/loi/tres20

Evapotranspiration monitoring with Meteosat Second Generation satellites: improvement opportunities from moderate spatial resolution satellites for vegetation

N. Ghilain, F. De Roo & F. Gellens-Meulenberghs

To cite this article: N. Ghilain, F. De Roo & F. Gellens-Meulenberghs (2014) Evapotranspiration monitoring with Meteosat Second Generation satellites: improvement opportunities from moderate spatial resolution satellites for vegetation, International Journal of Remote Sensing, 35:7, 2654-2670, DOI: 10.1080/01431161.2014.883093

To link to this article: https://doi.org/10.1080/01431161.2014.883093

International Journal of Remote Sensing, 2014
Vol. 35, No. 7, 2654–2670, http://dx.doi.org/10.1080/01431161.2014.883093

Taylor & Francis
Taylor & Francis Group

Evapotranspiration monitoring with Meteosat Second Generation satellites: improvement opportunities from moderate spatial resolution satellites for vegetation

N. Ghilain*, F. De Roo, and F. Gellens-Meulenberghs

Department Research and Development, Royal Meteorological Institute, 1180 Brussels, Belgium

(*Received 6 September 2012; accepted 16 April 2013*)

The Satellite Application Facility on Land Surface Analysis proposes a land evapotranspiration (ET) product, generated in near-real time. It is produced by an energy balance model forced by radiation components derived from data of the Spinning Enhanced Visible and Infrared Imager aboard Meteosat Second Generation geostationary satellites, at a spatial resolution of approximately 3 km at the equator and covering Europe, Africa, and South America. In this article, we assess the improvement opportunities from moderate spatial resolution satellites for ET monitoring at the Meteosat Second Generation satellite scale. Four variables, namely the land cover, the leaf area index (LAI), the surface albedo, and the open water fraction, derived from moderate-resolution satellites for vegetation monitoring are considered at two spatial resolutions, 1 km and 330 m, corresponding to the imagery provided by Satellite Pour l'Observation de la Terre (SPOT)-VEGETATION and future Project for On-Board Autonomy – Vegetation (PROBA-V) space-borne sensors. The variables are incorporated into the ET model, replacing or complementing input derived from the sensor aboard the geostationary satellite, and their relative effect on the model output is analysed. The investigated processes at small scales unresolved by the geostationary satellite are better taken into account in the final ET estimates, especially over heterogeneous and transition zones. Variables derived from sensors at 250–300 m are shown to have a noticeable effect on the ET estimates compared to the 1 km resolution, demonstrating the interest of PROBA-V 330 m-derived variables for the monitoring of ET at Meteosat Second Generation resolution.

1. Introduction

Evapotranspiration (ET) is a key component of the water cycle. Water is re-emitted into the atmosphere through direct evaporation of surface water, bare soils, and transpiration of plants. Alongside, the ET process causes a cooling of the land surface, as it consumes part of the energy stored by the surface. Therefore, ET plays an important role in both meteorological and hydrological processes. With the increasing demand for ET monitoring in a broad range of applications, including water management and agriculture, more and more techniques have been developed, and some automated. However, its monitoring is still a challenge as no direct observation is possible at the large scale (Dolman and De Jeu 2010), and only a combination of modelling and observations can help achieve that objective. Space-borne remote sensing has therefore been considered as a great opportunity to bypass the need of local observation, especially in poorly sampled regions.

*Corresponding author. Email: nicolas.ghilain@meteo.be

Recently, EUMETSAT's Satellite Application Facility on Land Surface Analysis, LSA-SAF (Trigo et al. 2011), has started the distribution of two near-real-time products aiming at ET monitoring: instantaneous every half-hour (MET) and daily cumulated, over the full field of view of the Spinning Enhanced Visible and Infrared Imager (SEVIRI) on board the geostationary satellite Meteosat Second Generation (MSG). It covers Europe, Africa, and Eastern South America (Ghilain, Arboleda, and Gellens-Meulenberghs 2011). ET is monitored at an unprecedented rate of one image every half-hour and is delivered through an operational continuous service provided by LSA-SAF host centre in Lisbon (http://landsaf.meteo.pt).

As it is based on geostationary satellite data, the spatial resolution becomes coarser towards the high viewing angles, with a resolution of 4–5 km over most of Western Europe. Given that spatial resolution, small-scale processes are unresolved, although their contribution might be not negligible to the total areal ET. Besides, information with an increased sub-grid resolution can help increase the accuracy of ET.

New products derived from remote sensing at moderate spatial resolution are now available and make a synergy possible with the coarse resolution information from MSG. However, in the context of continuous monitoring, it is recommended to have access to long data time series provided by continuous services. In that perspective, with its BioPar division, Geoland2 has begun providing (Lacaze et al. 2010) a service of continuous production of land-related variables (http://www.geoland2.eu). Satellite Pour l'Observation de la Terre – VEGETATION (SPOT-VGT) plays a major role in the production of such variables, as two successive SPOT satellites allow a continuous global monitoring of vegetation for about 15 years, at a spatial resolution of approximately 1 km. However, in 2013 the expected lifetime of the satellite will be exceeded. Its foreseen successor in the framework of the Global Monitoring for Environment and Security programme, Sentinel-3, designed to monitor globally vegetation at a spatial resolution of 300 m during seven years, is not expected to be exploited before 2014, leaving a gap in the continuous monitoring. The Project for Onboard Autonomy (PROBA-V) mission has therefore been set up to act as a gap-filler mission (Van Achteren et al. 2012), with sensors with about the same characteristics as SPOT-VGT, an expected lifetime of 2.5 years, and an enhanced spatial ground resolution of 330 m. Therefore, continuous service is secured, and spatial resolution is improved. In addition, the relatively high revisiting frequency of PROBA-V (global coverage once a day) makes its future data potentially interesting in terms of stability and reliability, valuable for operational production. The interest in the variables derived from moderate-resolution space-borne sensors and the benefits that could be obtained from the enhanced spatial resolution are particularly relevant for ET monitoring. The objective of this study is therefore to investigate the interest in complementing the ET model based on MSG with variables derived from 250 to 1000 m spatial resolution sensor imagery. Especially, we focus on the impact of four different variables derived from such imagery: land cover, leaf area index, waterbodies fraction, and land-surface albedo. Land cover is examined on the geolocation accuracy aspect: we assess further previous findings showing the reduced effects of an increase in the spatial resolution of satellite imagery on ET simulations at a few kilometres scale (Ghilain and Gellens-Meulenberghs forthcoming).

In the present article, we briefly describe the ET model, review the various products derived from moderate-resolution satellites that are of interest for the LSA-SAF ET products (Section 2), present the study sites and methods (Section 3), and assess their respective impact on test cases (Section 4). Finally, we provide a general conclusion and draw some perspectives towards the forthcoming launch of PROBA-V from the enhanced spatial resolution point of view (Section 5).

2. Model and data

2.1. LSA-SAF ET: model and output

The LSA-SAF proposes two ET variables-products: the instantaneous actual ET rate, MET, and the daily cumulated actual ET. Maps have been operationally and continuously produced since September 2009 and cover Africa, Europe, and part of South America, at the MSG/SEVIRI spatial resolution. The ET model implemented to derive the variables-products is an energy balance model (Ghilain, Arboleda, and Gellens-Meulenberghs 2011) fed by remote-sensing-derived products for radiation (Geiger, Carrer, et al. 2008; Geiger, Meurey, et al. 2008; Trigo et al. 2010), the daily land-surface albedo derived from MSG and short-term numerical weather forecasts from the European Centre for Medium-range Weather Forecasts. Land-cover information, and decomposition of vegetation classes into the model plant functional types, is needed to assign specific model parameters related to the maximum ET rate, and is currently provided by ECOCLIMAP-I, derived from one year NDVI Advanced Very High Resolution Radiometer (AVHRR) data, at 1 km resolution (Masson et al. 2003). In addition, the vegetation state, characterized by the leaf area index, LAI, and the fractional vegetation cover, FVC, are assigned using the ECOCLIMAP-I database. A new version of the MET algorithm, noted here V1, is a variant of the same model, including the use of other daily LSA-SAF products, i.e. LAI, FVC, and snow cover, following the methodology described in Ghilain et al. (2012). The variables derived from remote sensing used in the model are listed in Table 1. A schematic of the model is shown in Figure 1: the connections of the variables derived from the 300–1000 m imagery examined in this study with the different steps of the model and definition of input are highlighted. Those variables influence the ET model at different steps: the evaluation of plant functional-type-dependent canopy resistance to transpiration, the estimation of the aerodynamic resistance of the lower atmosphere to the vertical transfer of moisture, the calculation of the net radiation at the surface, and the surface heat fluxes computed iteratively until convergence. In addition, the weights of the different plant functional types and land uses needed to provide an areal composite of ET are also affected.

The model has been validated over Europe and Africa, by comparison with *in situ* measurements and inter-comparison with other models (Ghilain, Arboleda, and Gellens-Meulenberghs 2011).

Table 1. Variables and satellite-derived products used by the LSA-SAF evapotranspiration model.

Name	Variable	Sat.-Sensor	Resol. (km)	Frequency
ECOCLIMAP-I	Land-cover map	NOAA/AVHRR	1	Fixed
LSA-SAF LAI*	Leaf area index	MSG/SEVIRI	3.1†	Daily
LSA-SAF FVC*	Fractional vegetation cover	MSG/SEVIRI	3.1†	Daily
LSA-SAF SC2*	Snow cover characterization	MSG/SEVIRI	3.1†	Daily
LSA-SAF AL	Surface albedo	MSG/SEVIRI	3.1†	Daily
LSA-SAF DSSF	Shortwave radiation reaching the surface	MSG/SEVIRI	3.1†	30 min
LSA-SAF DSLF	Longwave radiation reaching the surface	MSG/SEVIRI	3.1†	30 min

Notes: *Used only by version V1 of the model. †Corresponds to the geostationary sub-satellite ground resolution.

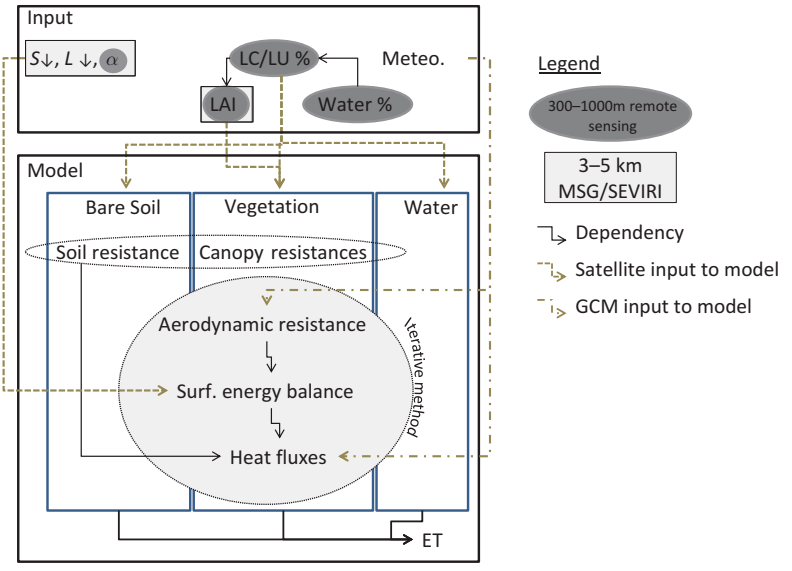

Figure 1. Schematic of the model steps and input. The process is shown for one model unit, with a differentiation between input provided by the global circulation model (GCM) ECMWF, the variables derived from the SEVIRI sensor aboard the geostationary MSG satellite, and finally the complementary variables derived from 300 m to 1000 m spatial resolution imagery from sensors aboard polar satellites examined in this study. $S_{\downarrow}$ and $L_{\downarrow}$ are, respectively, the shortwave and longwave radiation reaching the surface, α is the surface albedo, $LU/LC\%$ is the fraction of each plant functional type within a model unit given by the land-cover map, and Water$\%$ is the fraction of open water surface given by satellite-derived products.

2.2. *SPOT-VGT and PROBA-V instruments*

The VEGETATION programme is composed of a suite of two nearly identical sensors on board two satellites SPOT 4 and 5; it has been monitoring vegetation on the Earth's surface every 10 days since 1998. The satellites are on a Sun-synchronous orbit, with a time pass at 10:30, at 830 km from the ground. The sensor acquires one image per day for locations beyond 35° and five every six days for equatorial regions. The sensor acquires data in four spectral bands: blue (0.43–0.47 μm), red (0.61–0.68 μm), near infrared (0.78–0.89 μm), and short-wave infrared (1.58–1.75 μm). The ground spatial resolution is 1.15 km at nadir and 1.7 km on the sides, with a swath width of 2200 km.

The PROBA-V satellite is expected to be launched in 2013. Most of the characteristics from VEGETATION sensor acquisition are maintained as it is considered as a continuation mission. The satellite will fly at 820 km from the ground, the time pass will be maintained between 10:30 and 11:30, and there will be one acquisition every day, except for equatorial areas, with 90% coverage every day. Spectral bands and swath width are similar to VEGETATION. A major change in the characteristics is the ground spatial resolution, as it will be 330 m in average, with 100 m resolution at the centre of the swath and 350 m on the sides for the first three bands, and twice for the short-wave infrared. Both systems are expected to be characterized by the same relative geolocation accuracy.

2.3. *Variables of interest derived from moderate spatial resolution space-borne sensors*

Two pools of variables derived from moderate-resolution satellites are of interest for the improvement of ET monitoring in the LSA-SAF context. First are variables with the potential to improve the reliability of the results by a gain in spatial resolution. More specifically, those are variables already retrieved from MSG/SEVIRI, but their increased spatial resolution can lead to a more accurate estimation by spatial aggregation. Then are variables allowing the detection of unresolved features by MSG/SEVIRI. In the first pool, the land-cover map, the biophysical parameters describing the vegetation and the land-surface albedo are envisaged candidates. The second pool is composed of the small waterbodies and regularly flooded areas' detection.

For each variable of interest, the two ground spatial resolutions of SPOT-VGT and PROBA-V are required to evaluate the gain from using data from higher spatial resolution sensors to complement the ET model at a coarse scale. The lower product resolution corresponding to SPOT-VGT is 1 km. For this preparatory study in view of the PROBA-V launch, other similar remote-sensing-derived products are used to surrogate the future data, and the higher product resolution corresponding to PROBA-V varies between 250 and 500 m depending on the finest global product available.

2.3.1. *Land-cover map*

Because the land-cover map is the second most influential input on the modelled ET (Kato et al. 2007), an optimal choice has to be taken in order to comply with the necessary conditions for continuous monitoring. New global- or continental-scale land-cover maps have emerged using more recent remote-sensing data and longer time series. As an example, ECOCLIMAP-II has been developed on the basis of SPOT-VGT data (Tchuenté et al. 2011), at 1 km resolution over Africa, with a better accuracy than ECOCLIMAP-I owing to a multi-year analysis of the SPOT-VGT normalized difference vegetation index (NDVI) data. GlobCover v2.2 has been derived from Medium Resolution Imaging Spectrometer (MERIS) data at an enhanced resolution of 300 m (Bicheron et al. 2008). The MODIS land-cover map (MCD12Q1) is derived yearly from MODIS data and is available at 500 m spatial resolution. Each land-cover map is provided with a legend: it allows the decomposition of the classes into plant functional types used by land-surface models, and therefore ensures compatibility with the LSA-SAF ET model. In this study, the land-cover maps considered are ECOCLIMAP-I and GlobCover at 1000 and 300 m resolutions, respectively. Different aspects of the land-cover maps are relevant for the LSA-SAF model: the quality of the land-use classification, the geolocation accuracy, and the continuity of a series of updated land-cover maps. In a recent study (Ghilain and Gellens-Meulenberghs forthcoming), we have shown that the use of a land-cover map at 330 m allowed reduction of geolocation uncertainty on ET at the meso-scale compared to land-cover maps produced from 1 km data. The effect is particularly visible for spatial resolutions from 1 to 5 km. The LSA-SAF model is concerned with resolutions such as 3.1 km over Western Africa, 4–5 km over most of Europe, and up to 10 km over northern Scandinavia, Russia, and part of South America. Therefore, we study the effect of this geolocation uncertainty on ET produced with MSG/SEVIRI data over Europe.

2.3.2. *Leaf area index*

The biophysical parameter LAI is essential to the ET model, as it scales the transpiration process from a single leaf unit to the landscape level. In addition, in several models or

databases (Masson et al. 2003), LAI is associated with FVC by means of an exponential relation. The latter variable is used to determine the portion of land occupied by bare soil, and allows computing separately bare soil evaporation and plant transpiration. Available LAI products at moderate resolution are derived from MODIS at 1 km, e.g. MCD15 (Tian et al. 2000), and from SPOT-VGT at the same resolution, e.g. CYCLOPES LAI product (Baret et al. 2007). Recent advances have been made to derive LAI at higher resolution using MERIS 300 m (Bacour et al. 2006) or MODIS 250 m (Kouadio et al. 2012). Using such high-resolution LAI in the LSA-SAF ET model has proved beneficial in estimating more accurate ET rates over a winter wheat field in Belgium (Sepulcre-Cantó et al. 2013). A further assessment is proposed here using LAI from SPOT-VGT and MODIS at 1000 and 250 m, respectively.

2.3.3. *Waterbodies*

ET is known to be much higher over open waterbodies than over vegetated areas. Whereas permanent waterbodies are usually mapped and used in land-surface model applications, seasonal/eventual waterbodies, such as ponds and flooded plains, are scarcely represented, casting inevitable errors on the model estimates. Although sensors at MSG/SEVIRI spatial resolution have shown the possibility of detecting flooded areas in Africa (Proud et al. 2011), they could hardly detect small-sized waterbodies, and high-resolution sensors between 250 and 1000 m offer a more adequate imagery to monitor those seasonal surface waterbodies (Gond et al. 2004). Such small waterbodies and regularly flooded areas' regularly updated maps are therefore useful inputs for the LSA-SAF ET model. Gond et al. (2004) developed a method to detect small waterbodies and flooded areas from SPOT-VGT using NDVI and NDWI indices. More recently, Pedinotti et al. (2012) used MODIS/Terra NDVI and band 5 atmospherically corrected reflectance at 500 m resolution to monitor the surface water in the Sahel. In this study, NDVI and NDWI retrieved from SPOT-VGT and MODIS are used to derive the fraction covered by waterbodies at 1000 and 250 m, respectively.

2.3.4. *Land-surface albedo*

Since the ET model is an energy balance model, radiation components are required, and, in particular, the land-surface albedo. The surface albedo is an important term to compute the energy available at the surface for evaporation. Surface albedo generally differs among different land uses. In the model, ET is computed for each land-use class defined in the model, but the surface albedo is the same for all classes belonging to the very same MSG/SEVIRI pixel. One albedo for each sub-pixel land-cover type would change the local energy budget, and potentially affect the ET calculation. Although assuming a single albedo for every vegetation type belonging to an MSG pixel may be fully valid for mixed landscapes, homogeneous at MSG resolution, it could possibly be uncertain for heterogeneous areas, fragmented landscapes, and transition zones, and it could induce there a noticeable effect on ET. Using higher spatial resolution albedo allows the estimation of an albedo aggregated by vegetation type, necessary to compute the surface energy balance for each sub-pixel type. Ten days composites of the land-surface albedo from SPOT-VGT at 1 km are now available, as well as at 500 m and 1 km from MODIS. The products at 1000 and 500 m derived from SPOT-VGT and MODIS are used in this study.

Table 2. Variables and satellite-derived products used in our study.

	Product resol. 1			Product resol. 2		
Variable	Name	Sat.-Sensor	Resol. (km)	Name	Sat.-Sensor	Resol. (m)
Land cover	ECOCLIMAP	AVHRR	1	GlobCover v2.2	MERIS	300
Leaf area index	CYCLOPES	SPOT-VGT	1	MOD13Q1	MODIS-Terra	250
Albedo	Geoland2	SPOT-VGT	1	MCD43A3	MODIS-Terra/ Aqua	500
Waterbodies	Geoland2 NDVI	SPOT-VGT	1	NDVI	MODIS-Terra	500
	Geoland2 NDWI	SPOT-VGT	1	Reflectance	MODIS-Terra	500

Table 2 lists the products whose utilities are explored in the context of the LSA-SAF MET algorithm, bearing in mind the continuity secured by the suite composed by SPOT-VGT and PROBA-V satellites.

3. Study sites and methods

The optimal demonstration of the effect of each considered variable is expected in different conditions depending on the variable. Therefore, the present study does not focus on a standardized methodology for assessing the impact on the LSA-SAF ET. The study sites (Figure 2) specific to each variable are described here, as well as the method employed to show the impact on the resulting ET estimates.

To assess the impact of geolocation uncertainty of land-cover map on the ET estimation, we have focused on Europe, which is expected to be more affected by it. Land-cover maps at two spatial resolutions, 1000 and 300 m, are needed to assess the difference between maps derived from SPOT-VGT and PROBA-V. To separate the effect of geolocation accuracy with the misclassification arising due to different methodologies or sensor characteristics, we chose to use the GlobCover land-cover map at 300 m and an aggregated version at 1 km, called the reference maps. Given that the absolute geolocation accuracy is one pixel for both SPOT-VGT and PROBA-V, both maps are shifted by one pixel, and called shifted maps. The difference between the reference and the shifted map is a measure of the effect of geolocation error on the land-cover map input in the model. To assess the impact on ET, the maps are aggregated at the coarser variable MSG/SEVIRI resolution in view of their use in the LSA-SAF model. Each class of GlobCover is decomposed into three broad vegetation types – high vegetation, low vegetation, and other types. To evaluate the impact on the ET model, we have derived a function to approximate the relation between the error on the change of percentage of forested areas to low vegetation, based on the findings of Ghilain and Gellens-Meulenberghs (forthcoming). Using this relation, land-cover change $\Delta LC_{\%}$ is converted into relative error on ET $\Delta_{\%}ET$.

$$\Delta_{\%}ET = 0.1560 + 0.1167\Delta LC_{\%} - 0.002\Delta LC_{\%}^{2}. \quad (1)$$

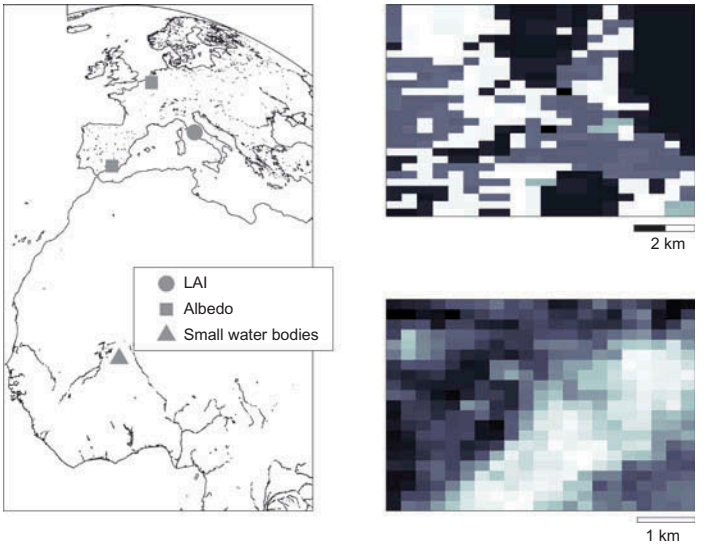

Figure 2. The sites in Europe and Africa used in this study in the projection of MSG/SEVIRI (left). Focus on two sites used: (top) the land-cover types (sparse vegetation, irrigated, and rain-fed crops) from GlobCover at the Spanish site, (bottom) MODIS NDVI during Summer 2007 at the Italian site revealing an oblique narrow band of forest within the agricultural landscape.

As mentioned in Section 2, LSA-SAF MET takes input from the ECOCLIMAP-I database for vegetation phenology. The new variant V1 leverages the recent LSA-SAF LAI product, available at MSG/SEVIRI spatial resolution. However, in patchy landscapes, a statistical post-processing procedure needs to be applied, using vegetation signals from distant neighbour pixels. A high-resolution land-cover map (GlobCover) is used along with CYCLOPES LAI (1 km) derived from SPOT-VGT and MOD13Q1 (250 m) derived from MODIS/Terra for the year 2007. The MOD13Q1 product offers NDVI at 250 m, but there is no available LAI product at such a resolution. Therefore it is necessary to convert into LAI time series, accepted by the energy balance model. Different methods have been under focus. The method of Lu and Shuttleworth (2002) that proceeds by cumulative distribution matching reduces the difference in LAI that can occur due to a difference in the LAI retrieval algorithms. Such a *processed* difference should be distinguished from a *physical* difference in LAI, which is instead the result of a better characterization of the surface, e.g. due to an increased spatial resolution or a more precise time sampling of the annual evolution of the vegetation. Because of that limitation, another method was used. From the match of SPOT-VGT NDVI to CYCLOPES LAI, we derive an exponential function that is used to convert MODIS NDVI into LAI at 250 m resolution. We aggregate the LAI by vegetation types within an MSG/SEVIRI pixel making using the land-cover map (Figure 3) and then limit the number of spatial units to run the model. The surface roughness parameters required by the model are derived from the LAI obtained using the formulation of ECOCLIMAP-I. This method has been applied over a particular site in Roccarespampani, Italy (42.41° N, 11.93° E), composed of a deciduous forest (Quercus cerris) and crops. The site is equipped with an eddy correlation device that measures the fluxes of heat and moisture from the underlying surface, mostly represented by the forest (Tedeschi et al. 2006).

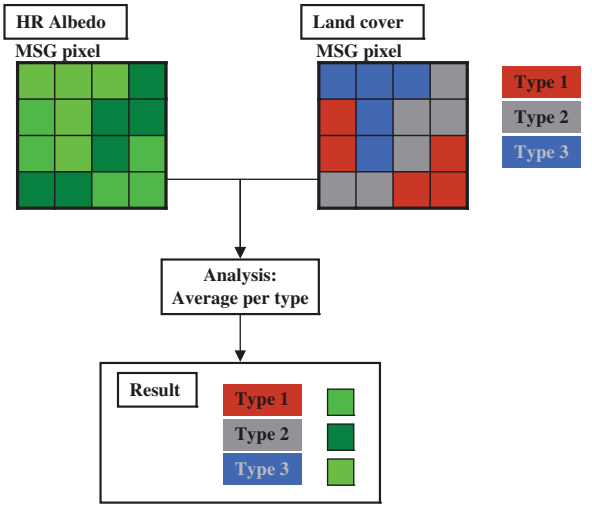

Figure 3. Aggregation methodology to obtain one albedo per vegetation type at the selected MSG/SEVIRI pixel from moderate-resolution variable-product: a land-cover map is used to discriminate the albedo values per vegetation class before averaging. The same methodology is applied to obtain aggregated time series of LAI.

As surface albedo can be estimated from moderate-resolution satellites (250–1000 m), it is theoretically possible to create an average albedo for each vegetation class inside an MSG pixel, using the methodology depicted in Figure 3, but using albedo instead of LAI. Because the effect is expected to be most sensible in heterogeneous and transition zones, we focus on two areas with contrasted land uses. Both areas have been chosen for their different climate and known contrasts: east of Brussels (50.81° N, 4.59° E) and south of Spain (37.35°N, 3.18°W), and have an extent of 3 × 3 MSG pixels. The region east of Brussels is composed of urban areas, as well as deciduous forests (beech stands), and croplands (mostly sugar beets and wheat). Those three tiles are well localized. The Spanish region is composed of irrigated crops, annual crops, and sparse woodland, mainly. For the construction of the 'tile' albedo time series, HR (SPOT-VGT or MODIS) albedo is selected according to the land covers, i.e. GlobCover v2.2, MODIS, and ECOCLIMAP-I. Using separately each land cover to tag the albedo values does not result in reliable results, because of the land-cover map discrepancies found in the selected areas. Moreover, a per-pixel analysis does not seem useful (results not shown here), so an analysis on a 3 × 3 MSG pixel area has been conducted. A way to bypass the problem of land-cover mismatch is to use simultaneously the land covers, and use only the pixels with acceptable agreement between land-cover maps to derive the 'tile' values. For the Belgian region, the best match is between MODIS LC and GlobCover (bare areas are set to be agricultural land), and for the Spanish region, ECOCLIMAP-I matches with GlobCover. Mean time series of cropland and forest albedos are retrieved for the Belgian region. For the Spanish region, time series are retrieved and aggregated for both types of crops, irrigated (15%) and non-irrigated (10%), and for sparse woodland (73%). The ET model has then been modified to accept not only one pixel albedo from LSA-SAF, but an albedo estimate for each tile.

To show the effect of waterbody detection by moderate-resolution sensors for vegetation, we focus on a specific Sahelian region in Mali, known to be covered with seasonal

ponds during and after the West African monsoon (Timouk et al. 2009). The region is of special interest, because, in the framework of an international project aiming at understanding the mechanism of the West African monsoon (Redelsperger et al. 2006), devices have been installed to measure on flux towers the exchanges of energy between the surface and the atmosphere (Mougin et al. 2009). Of particular interest in the present context are the observations of ET at the Kelma site (15.22° N, 1.57° W), monitoring a forested area (acacia trees) situated in a clay depression, where ponds are observed from July to January approximately. Seasonality is strong in that area, and small clay depressions collect the run-off during the rainy period. The ponds created slowly evaporate during the dry season. The highest measured ET is connected with vegetation growth, but as the vegetation senescence begins, high ET rates are still measured. Such high ET rates without a full vegetation cover can only be attained by the direct evaporation from waterbodies. LSA-SAF ET results are known to be deficient over that specific location, probably because of the seasonal ponds not taken into account in the ET modelling. We consequently investigate here the possibility of improving the ET estimates on that specific location using remote-sensing products able to detect open water surfaces. It is possible to monitor the small waterbodies using NDVI and NDWI derived from SPOT-VGT at 1 km (Gond et al. 2004). The threshold method has been applied on a set of NDVI and NDWI images derived from SPOT-VGT and MODIS for the period from November 2009 to October 2010 over a region of 25 km^2 around Kelma in Mali. Higher resolution should provide more accurate estimation of the fraction of open waterbodies, as it can detect smaller water surface than at 1 km, and, at least, it provides a more robust statistical NDWI mean over the area for use in the 'threshold' method of Gond et al. (2004). The LSA-SAF ET model has been slightly modified to accept as input a map of fraction of surface water, and reprocessing of year 2007 has been applied to obtain a new time series of ET over the Kelma station, using the series of fraction of surface water derived from MODIS.

4. Impact on LSA-SAF ET

The effect on the LSA-SAF ET of each considered variable is detailed in separate subsections.

4.1. Land-cover maps

At MSG/SEVIRI resolution, the error on the forest fraction due to geolocation uncertainty is variable as expected with the viewing angles of the geostationary satellite: the largest errors are found where the viewing angle is the smallest. A mean and a maximum error in forest fraction within a region of 25 neighbouring pixels are represented in Figure 4 for both maps at 300 and 1200 m. Some regions are not much affected by the shift in the land-cover maps, whereas others can reach mean values of 2% and 10% for the 300 and 1200 m maps, respectively. When examining the maximum change within each 25-pixel region, an error of 6% and 30% is observed over Spain for, respectively, both resolutions.

The impact on ET also depends on the viewing angle and the spatial resolution of the used land-cover map as seen in Figure 5. The relative error on ET is about 1% when using a land-cover map at 300 m (Figure 5(*a*)), whereas the use of the 1200 m map generates a relative error ranging up to 5% at some locations (Figure 5(*b*)). It is therefore expected to reach a better confidence level in the ET results over Spain, Italy, and Southern France if using a land-cover map generated from PROBA-V.

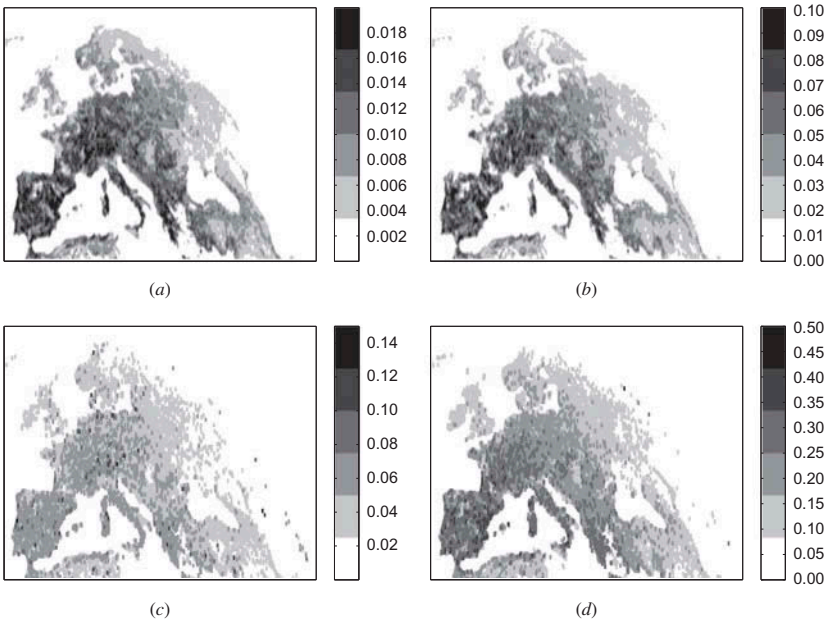

Figure 4. Mean uncertainty on 25 neighbouring pixels at MSG/SEVIRI resolution in the forest fraction over Europe due to geolocation error on land-cover maps at 300 m and 1200 m spatial resolution (*a*) and (*b*). The distribution of the maxima over each 25 neighbouring pixels is shown in (*c*) and (*d*).

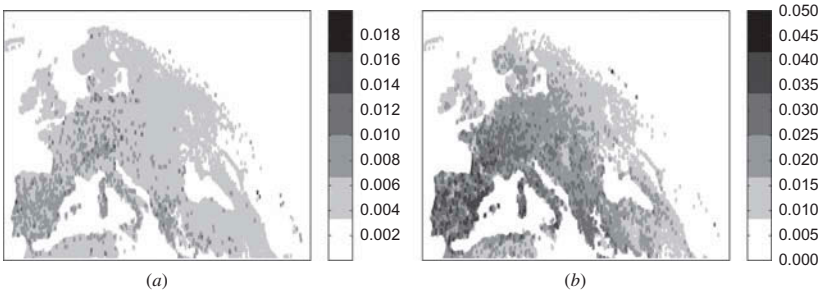

Figure 5. Relative difference in evapotranspiration due to geolocation uncertainty of 300 m (*a*) and 1200 m (*b*) land-cover maps.

4.2. Leaf area index

The retrieved LAI time series from SPOT-VGT (CYCLOPES) and MODIS for the two dominant vegetation types at Roccarespampani site show differences in the amplitude and timing of the full canopy cover characterizing the deciduous forest (Figure 6(*a*)), whereas there is an agreement for the crop class phenology. This observed difference in the retrieved LAI impacts the ET estimated by the LSA-SAF model, with higher daily rates for the forest using the 250 m product aggregated to MSG/SEVIRI resolution (Figure 6 (*b*)). However, at the coarse pixel scale, because the forest occupies a mere 10–12% of the pixel area, the difference is still noticed but greatly reduced (Figure 7). Compared to the

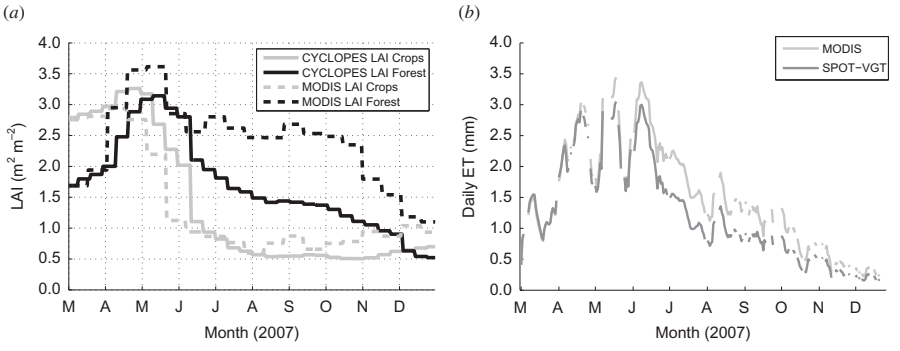

Figure 6. Leaf area index time series aggregated from the 1 km and the 250 m imagery over Roccarespampani, and their effect on the evapotranspiration estimation over the forest.

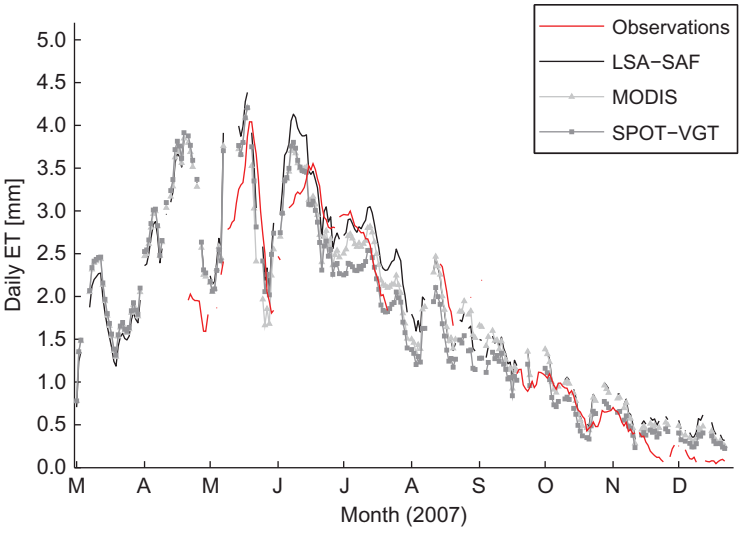

Figure 7. Comparison of the model daily evapotranspiration to *in situ* observation at the Roccarespampani site. The control output has been produced using LSA-SAF model V1, and the two other simulations with SPOT-VGT and MODIS LAI, respectively. The evapotranspiration estimates are representative of the MSG/SEVIRI pixel encompassing the site.

ET model V1 output, most changes occur during the summer months for which the estimates using the 250 m LAI are slightly closer to the *in situ* daily cumulated observations (July). This could indicate that the LAI series at 250–300 m resolution could have a beneficial impact, although minor, on ET simulations at the MSG scale compared to the series obtained at 1 km, especially in such transition (crop/forest) areas. It should be noted here that part of the observed difference between observations and model estimates is due to different representativities: observations are representative of the forest, whereas the model estimates are representative of a surface dominated by crops. However, Figure 5 shows that the LSA-SAF model might have some difficulties in simulating the observed ET rates in April. However, the use of 250 m or 1000 m LAI does not allow correcting the model deficiency.

4.3. Land-surface albedo

For the Spanish region, the maximum contrast is expected from the separation between annual crops and irrigated crops. The albedo time series retrieved from MODIS for both crop types are shown in Figure 8(*a*), along with the LSA-SAF albedo product. The albedo retrieved from MODIS for the sparse forest (not displayed) is very similar to the irrigated tile albedo. No series is shown for Geoland2 series as no clear separate signals could be found for each land-use class, showing the potential limitation of 1 km data for such types of landscapes. Mean values are represented as continuous lines, whereas the shaded areas are bounded by the maxima and minima of each sample. LSA-SAF albedo agrees with MODIS albedo in the studied areas: the global annual cycle is similar and the estimates are in the same range of magnitude. The 'tile' albedo time series can be, however, different. For the Spanish area, the difference can be as large as 0.07 between the two types of crops in July and August, with an albedo 30% lower for irrigated crops than for annual crops. For the Belgian area, snow is detected in December 2009 and January 2010 and the highest difference observed, except for the snow event, is about 0.02, i.e. 10% (not shown), leading to almost no change in ET estimation. It must be mentioned here that the weighted contribution of the 'tile' albedos derived from MODIS follows fairly well the averaged LSA-SAF albedo for the study sites.

The result of the ET model V1 is considered as the control simulation for the area in Spain, where albedo from high resolution is expected to affect ET estimates at the MSG scale. The effect of using an albedo assigned with MODIS for each vegetation type of the coarse model unit is seen by comparison with the simulation results from the modified ET model for which a relative difference between daily ET is calculated (Figure 8(*b*)). As expected, ET is affected by the tile albedo values. Apart from the winter peak, which leads to very little change in ET rates, the difference has a seasonal cycle with the largest difference during the summer season. Daily ET cumulates are lower by 15–20% using the MODIS albedo. This is an effect of the use of tile albedos in the model, especially caused by the higher albedo found for annual crops, which allows less energy at the surface to be used for turbulent transfers with the atmosphere.

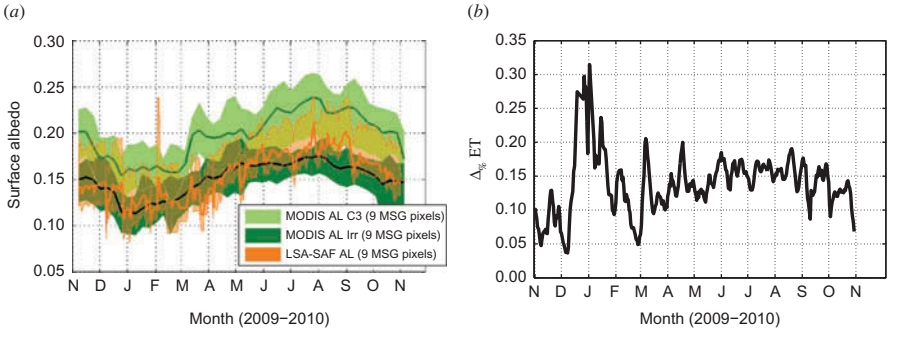

Figure 8. Surface albedo time series aggregated from MODIS imagery over the test area, and the effect of a vegetation-type-dependent albedo on the total daily evapotranspiration estimation over the study site. (*a*) Surface albedo time series for the test area in Spain for a group of 3 × 3 MSG/SEVIRI pixels: LSA-SAF albedo (orange), vegetation type MODIS derived albedo (dark green for irrigated (Irr) tile and light green for annual (C3) crops). Albedo for sparse forests (not displayed) is similar to the albedo of irrigated crops. Maximum, minimum and mean area sample are presented. (*b*) Relative difference between daily ET cumulates (5 days sliding average) $\Delta_{\%}$ ET estimated by the LSA-SAF model in its nominal configuration (with the LSA-SAF albedo) and in the variant accepting albedo from MODIS.

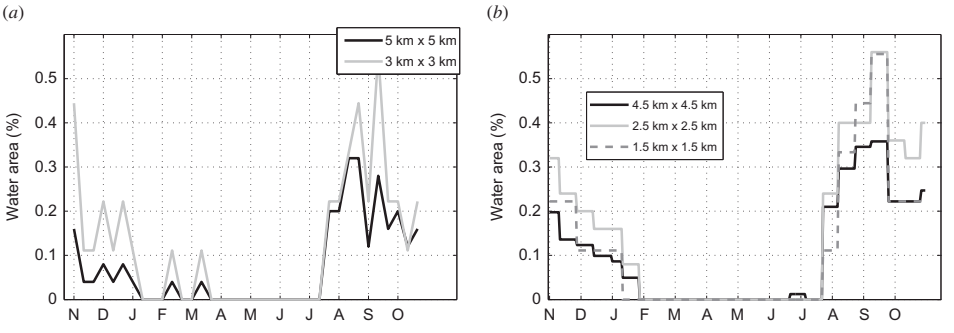

Figure 9. Comparison of the time series of small waterbodies fraction cover over the Kelma site as derived from SPOT-VGT and MODIS over November 2009–October 2010. (*a*) Time series retrieved from SPOT-VGT NDVI and NDWI using different averaging windows, and (*b*) time series retrieved from MODIS NDVI and NDWI using different averaging windows.

4.4. Small waterbodies and flooded areas detection

The time series of open waterbodies fraction obtained from SPOT-VGT and MODIS exhibit similar seasonality for the period from November 2009 to October 2010 (Figure 9), with an abrupt apparition of large portions ($\geq$20%) of the land surface occupied by waterbodies during July, and a progressive evaporation of this water from September to February. The information derived from the 250 m remote-sensing data is however more stable, probably owing to the increased size of the sample used for averaging. For both remote-sensing resolutions, differences in the waterbodies percentage are observed for various sizes of the averaging window, showing a higher concentration of flooded areas centred on the Kelma site. Because of more stable time series derived from the imagery at 250 m, using such data to be input in the ET model is recommended. The time series of waterbodies fraction derived from MODIS data for the same site over the period from June to December 2007 exhibits approximately the same seasonality but is characterized by an abrupt increase showing up earlier at the beginning of July and a higher proportion of land flooded during the wet season (Figure 10(*a*)).

A comparison between *in situ* observation and both simulations using the LSA-SAF model V1 with and without the open water fraction for the period from June to December 2007 has revealed that the ET rate is more realistically estimated using the open water fraction derived from high-resolution satellites (Figure 10(*b*)). The fit is especially good for the beginning of the rainy season. A progressive decrease of the modelled ET from October to December is in agreement with the decrease in the percentage of waterbodies obtained from remote sensing. However, simulation at the MSG scale does not necessary fit the exact situation around the *in situ* measurement site, which can be affected by a higher percentage of flooded land than prescribed.

5. Conclusion and perspectives

Based on the test cases presented here, we have shown the utility of moderate-resolution satellites towards the improvement of the LSA-SAF ET products derived from MSG/SEVIRI. In particular, four different variables derived from moderate-resolution satellites for vegetation monitoring have been assessed regarding the LSA-SAF ET products. Processes at small scales unresolved by the geostationary satellite are better taken into account in the final ET estimates. The effect is particularly strong for the detection of

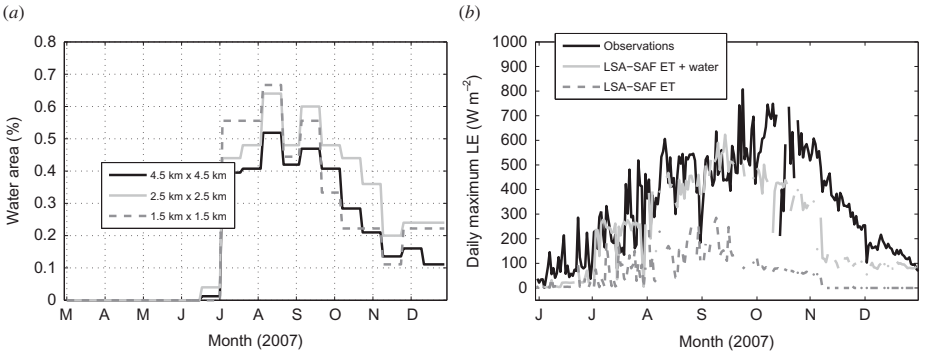

Figure 10. Kelma (Mali): taking into account the time series fraction of open water derived from the moderate-resolution sensor improves the monitoring of evaporation with the LSA-SAF model. (*a*) Same as in Figure 9(*b*), but for 2007. The series at 2.5 km is used for the evapotranspiration estimation, and (*b*) *in situ* observations against simulations of latent heat flux from LSA-SAF ET model VI in its nominal configuration, and using additionally the open water fraction derived from remote sensing.

small seasonal waterbodies that allows the model to better capture the observed dynamics. It is still seen but to a lesser extent for land-surface albedo, with differences in daily ET rates up to 20% in a contrasted site in southern Spain. However, LAI at higher resolution has a minor impact at the investigated site, possibly highlighting a weak dependence of the model in this variable. Effects of the increased spatial resolution of the moderate satellite imagery have been shown to be beneficial for ET estimations, especially for heterogeneous and transition areas. The variables derived from SPOT-VGT are therefore highly expected to be generated from its successor PROBA-V in view of the continuous time series it could offer to ET models at MSG/SEVIRI resolution.

With respect to spatial resolution from the complementary satellite, it has been highlighted that variables derived at 250–500 m improve better the LSA-SAF ET than do the 1 km-derived products. ET uncertainty arising due to geolocation errors in the land-cover map is reduced when a land-cover map at 300 m resolution is used, compared to the map at 1 km. More stable time series of waterbodies fraction can be retrieved from 250 m imagery compared to 1 km, and a better recognition of landscape patterns is observed at 250 m. This resolution allows an accurate aggregation of the biophysical and surface variables for each vegetation type at MSG/SEVIRI resolution. Consequently, sensors such as PROBA-V are expected to be an improvement compared to SPOT-VGT towards the use of their derived data in the LSA-SAF model and land-surface models at meso-scale resolutions. Moreover, an increased spatial resolution of the moderate satellite imagery is expected to be complementary to the future geostationary satellites Meteosat Third Generation, which are expected to monitor Europe and Africa at 1 km spatial resolution in replacement of the MSG suite of satellites.

Further work will focus on the applicability of integrating such variables derived from moderate-resolution sensors in the LSA-SAF ET model with respect to timeliness and long-term continuity for a proper monitoring of ET in near-real time.

Acknowledgements

This study is part of the PROBA-VET project (contract CB/34/18), part of the PROBA-V Preparatory Programme of the Belgian Science Policy. Products from MODIS have been acquired through the online Data Pool at the NASA Land Processes Distributed Active Archive Center (LP

DAAC), USGS/EROS Center (http://lpdaac.usgs.gov/getdata). GlobCover v2.2 has been distributed by MEDIAS-France (ESA GlobCover project). NDVI S10 from SPOT-VGT has been provided by VITO after registration on: http://free.vgt.vito.be/. CYCLOPES data set for 2007 has been provided through Postel MEDIAS-France. These products (LAI, NDVI, FAPAR, FCover) are the joint property of INRA, CNES, and VITO under copyright geoland2. They are generated from the SPOT VEGETATION data under copyright CNES and distribution by VITO. The BioPar albedo product was originally developed in the framework of the FP6/CYCLOPES project. It is generated from the SPOT VEGETATION data under copyright Cnes and distribution by VITO. The BioPar albedo is available at the address http://www.geoland2.eu.')

Funding

Geoland2 products have been provided through the Geoland2 access portal after registration. The research leading to these results has received funding from the European Community's Seventh Framework Programme (FP7/2007-2013) under grant agreement no. 218795.

References

Bacour, C., F. Baret, D. Béal, M. Weiss, and K. Pavageau. 2006. "Neural Network Estimation of LAI, fAPAR, fCover and LAI×Cab, from Top of Canopy MERIS Reflectance Data: Principles and Validation." *Remote Sensing of Environment* 105: 313–325. doi:10.1016/j.rse.2006.07.014.

Baret, F., O. Hagolle, B. Geiger, P. Bicheron, B. Miras, M. Huc, B. Berthelot, F. Niño, M. Weiss, O. Samain, J. Roujean, and M. Leroy. 2007. "LAI, FAPAR, and FCover CYCLOPES Global Products Derived from Vegetation. Part 1: Principles of the Algorithm." *Remote Sensing of Environment* 110: 275–286. doi:10.1016/j.rse.2007.02.018.

Bicheron, P., M. Huc, C. Henry, S. Bontemps, and GlobCover Partners. 2008. *GLOBCOVER: Products Description Manual*. PDM 2.2, AT&T Labs-Research. ESA. http://due.esrin.esa.int/globcover/

Dolman, A. J., and R. A. M. de Jeu. 2010. "Evaporation in Focus." *Nature Geoscience* 3: 296. doi:10.1038/ngeo849.

Geiger, B., D. Carrer, L. Franchistéguy, J. Roujean, and C. Meurey. 2008. "Land Surface Albedo Derived on a Daily Basis from Meteosat Second Generation Observations." *IEEE Transactions on Geoscience and Remote Sensing* 46: 3841–3856. doi:10.1109/TGRS.2008.2001798.

Geiger, B., C. Meurey, D. Lajas, L. Franchistéguy, D. Carrer, and J. L. Roujean. 2008. "Near Real-Time Provision of Downwelling Shortwave Radiation Estimates Derived from Satellite Observations." *Meteorological Applications* 15: 411–420. doi:10.1002/met.84.

Ghilain, N., A. Arboleda, and F. Gellens-Meulenberghs. 2011. "Evapotranspiration Modelling at Large Scale Using Near-Real Time MSG SEVIRI Derived Data." *Hydrology and Earth System Sciences* 15: 771–786. doi:10.5194/hess-15-771-2011.

Ghilain, N., A. Arboleda, G. Sepulcre-Cantò, O. Batelaan, J. Ardö, and F. Gellens-Meulenberghs. 2012. "Improving Evapotranspiration in a Land Surface Model Using Biophysical Variables Derived from MSG/SEVIRI Satellite." *Hydrology and Earth System Sciences* 16: 2567–2583. doi:10.5194/hess-16-2567-2012.

Ghilain, N., and F. Gellens-Meulenberghs. Forthcoming. "Impact of Land Cover Map Resolution and Geolocation Accuracy on Evapotranspiration Simulations by a Land Surface Model." *Remote Sensing Letters*.

Gond, V., E. Bartholomée, F. Ouattara, A. Nonguierma, and L. Bado. 2004. "Surveillance et Cartographie des Plans D'eau et des Zones Humides et Inondables en Régions Arides Avec L'instrument VEGETATION Embarqué Sur SPOT-4." *International Journal of Remote Sensing* 25: 987–1004. doi:10.1080/0143116031000139908.

Kato, H., M. Rodell, F. Beyrich, H. Cleugh, E. van Gorsel, H. Liu, and T. P. Meyers. 2007. "Sensitivity of Land Surface Simulations to Model Physics, Land Characteristics, and Forcings, at Four CEOP Sites." *Journal of the Meteorological Society of Japan* 85A: 187–204. doi:10.2151/jmsj.85A.187.

Kouadio, L., G. Duveiller, B. Djaby, M. E. Jarroudi, P. Defourny, and B. Tychon. 2012. "Estimating Regional Wheat Yield from the Shape of Decreasing Curves of Green Area Index Temporal Profiles Retrieved from MODIS Data." *International Journal of Applied Earth Observation and Geoinformation* 18: 111–118. doi:10.1016/j.jag.2012.01.009.

Lacaze, R., G. Balsamo, F. Baret, J. Calvet, F. Camacho, R. d'Andrimont, P. Pacholczyk, H. Poilvé, B. Smets, K. Tansey, I. Trigo, and W. Wagner. 2010. "Geoland2 – Towards an Operational GMES Land Monitoring Core Service: First Results of the Biogeophysical Parameters Core Mapping Service." In *Proceedings of the Abstract Book of the Recent Advances in Quantitative Remote Sensing (RAQRS): 3rd International Symposium*, Torrent, September 27–October 1, Torrent, 116 p.

Lu, L., and J. Shuttleworth. 2002. "Incorporating NDVI-Derived LAI into the Climate Version of RAMS and its Impact on Regional Climate." *Journal of Hydrometeorology* 3: 347–362. doi:10.1175/1525-7541(2002)003%3C0347:INDLIT%3E2.0.CO;2.

Masson, V., J. L. Champeaux, F. Chauvin, C. Meriguet, and R. Lacaze. 2003. "A Global Database of Land Surface Parameters at 1-km Resolution in Meteorological and Climate Models." *Journal of Climate* 16: 1261–1282. doi:10.1175/1520-0442-16.9.1261.

Mougin, E., P. Hiernaux, L. Kergoat, M. Grippa, P. de Rosnay, F. Timouk, V. L. Dantec, V. Demarez, F. Lavenu, M. Arjounin, T. Lebel, N. Soumaguel, E. Ceschia, B. Mougenot, F. Baup, F. Frappart, P. Frison, J. Gardelle, C. Gruhier, L. Jarlan, S. Mangiarotti, B. Sanou, Y. Tracol, F. Guichard, V. Trichon, L. Diarra, A. Soumaré, M. Koité, F. Dembélé, C. Lloyd, N. Hanan, C. Damesin, C. Delon, D. Serça, C. Galy-Lacaux, J. Seghieri, S. Becerra, H. Dia, F. Gangneron, and P. Mazzega. 2009. "The AMMA-CATCH Gourma Observatory Site in Mali: Relating Climatic Variations to Changes in Vegetation, Surface Hydrology, Fluxes and Natural Resources." *Journal of Hydrology* 375: 14–33. doi:10.1016/j.jhydrol.2009.06.045.

Pedinotti, V., A. Boone, B. Decharme, J. Crétaux, N. Mognard, G. Panthou, F. Papa, and B. A. Tanimoun. 2012. "Evaluation of the ISBA-TRIP Continental Hydrologic System over the Niger Basin Using In Situ and Satellite Derived Datasets." *Hydrology and Earth System Sciences* 16: 1745–1773. doi:10.5194/hess-16-1745-2012.

Proud, S. R., R. Fensholt, L. V. Rasmussen, and I. Sandholt. 2011. "Rapid Response Flood Detection Using the MSG Geostationary Satellite." *International Journal of Applied Earth Observation and Geoinformation* 13: 536–544. doi:10.1016/j.jag.2011.02.002.

Redelsperger, J. L., C. Thorncroft, A. Diedhiou, T. Lebel, D. Parker, and J. Polcher. 2006. "African Monsoon Multidisciplinary Analysis: An International Research Project and Field Campaign." *Bulletin of the American Meteorological Society* 87: 1739–1746. doi:10.1175/BAMS-87-12-1739.

Sepulcre-Cantó, G., F. Gellens-Meulenberghs, A. Arboleda, G. Duveiller, A. D. Wit, H. Eerens, B. Djaby, and P. Defourny. 2013. "Estimating Crop Specific Evapotranspiration Using Remote Sensing Imagery at Various Spatial Resolutions for Improving Crop Growth Modeling." *International Journal of Remote Sensing* 34 (9–10): 3274–3288.

Tchuenté, A. T. K., S. M. D. Jong, J. L. Roujean, C. Favier, and C. Mering. 2011. "Ecosystem Mapping at the African Continent Scale Using a Hybrid Clustering Approach Based on 1-km Resolution Multi-Annual Data from SPOT/VEGETATION." *Remote Sensing of Environment* 115: 452–464. doi:10.1016/j.rse.2010.09.015.

Tedeschi, V., A. Rey, G. Manca, R. Valentini, P. G. Jarvis, and M. Borghetti. 2006. "Soil Respiration in a Mediterranean Oak Forest at Different Developmental Stages after Coppicing." *Global Change Biology* 12: 110–121. doi:10.1111/j.1365-2486.2005.01081.x.

Tian, Y., Y. Zhang, Y. Knyazikhin, R. B. Myneni, J. M. Glassy, G. Dedieu, and S. W. Running. 2000. "Prototyping of MODIS LAI and FPAR Algorithm with LASUR and LANDSAT Data." *IEEE Transactions on Geoscience and Remote Sensing* 38: 2387–2401. doi:10.1109/36.868894.

Timouk, F., L. Kergoat, E. Mougin, C. R. Lloyd, E. Ceschia, J. M. Cohard, P. de Rosnay, P. Hiernaux, V. Demarez, and C. M. Taylor. 2009. "Response of Surface Energy Balance to Water Regime and Vegetation Development in a Sahelian Landscape." *Journal of Hydrology* 375 (1–2): 178–189.

Trigo, I. F., C. Barroso, P. Viterbo, S. C. Freitas, and I. T. Monteiro. 2010. "Estimation of Downward Longwave Radiation at the Surface Combining Remotely Sensed Data and NWP Data." *Journal of Geophysical Research* 115. doi:10.1029/2010JD013888.

Trigo, I. F., C. C. DaCamara, P. Viterbo, J.-L. Roujean, F. Olesen, C. Barroso, F. Camacho-de Coca, D. Carrer, S. C. Freitas, J. Garcia-Haro, B. Geiger, F. Gellens-Meulenberghs, N. Ghilain, J. Melia, L. Pessanha, N. Siljamo, and A. Arboleda. 2011. "The Satellite Application Facility on Land Surface Analysis." *International Journal of Remote Sensing* 32: 2725–2744. doi:10.1080/01431161003743199.

Van Achteren, T., W. Dierckx, S. Sterckx, S. Livens, and G. Saint. 2012. "Proba-V – A SPOT-VGT Successor Mission, Product Definition and Specifications." 32nd EARSEL Symposium Proceedings – Advances in Geosciences, Mykonos Island, May 21–24, 424–429.